

Flow-Induced Vibration Characteristics of a V-shaped Prism and Performance of Magnetostrictive Wind Vibrational Power Generator

Takahiro Kiwata¹, Takahito Hamano², Sotaro Takeuchi², Takuma Shima²,
Mohamed Heragy³, and Toshiyuki Ueno⁴

¹ School of Mechanical Engineering, Kanazawa University, Japan, kiwata@se.kanazawa-u.ac.jp

² Graduate School of Natural Sciences and Technology, Kanazawa University, Japan

³ School of Mechanical Engineering, Kanazawa University, Japan

⁴ School of Electrical and Computer Engineering, Kanazawa University, Japan

SUMMARY:

Wind tunnel test was carried out to develop a vibration-based power generator using magnetostrictive material from the flow-induced transverse vibration of a cantilevered prism having a V-shaped cross-section. We focused on transverse vortex-induced vibration (VIV) and the galloping vibration for a V-shaped prism. The effects of the height and the interior angle of V-shaped prisms having a span length of $L = 200$ mm on the vibration characteristics and the power extracted from the vibration generator were investigated. The height H and the interior angle β of the prism were changed from 20 mm to 60 mm, and from 60° to 150° , respectively. The maximum power generated by a V-shaped prism with $H = 50$ mm and $\beta = 90^\circ$ without a splitter plate is 5.02 mW. The effect of a splitter plate installed behind a V-shaped prism having a height of $H = 50$ mm was also investigated. The gap G between the splitter plate and the prism was changed from 8 mm to 104 mm. The splitter plate has an influence on the response amplitude for a V-shaped with $G/H = 0.2$, that is, it does not vibrate without an added initial displacement. The response amplitude of a V-shaped prism with $G/H \geq 1.2$ is similar to that without a splitter plate.

Keywords: Flow-induced vibration, Galloping, V-shaped prism, Splitter plate, Power generator

1. INTRODUCTION

Vibrational generators by using wind vibration and magnetostrictive material, i.e. Iron-gallium alloy, have attracted considerable attention for energy generation [Ueno and Yamada, 2011]. Such generators can serve as a power source to replace batteries for low-power sensors and wireless communication systems such as the Internet of Things (IoT) devices. Magnetostrictive materials exhibit an inverse magnetostrictive effect, i.e., the magnetic flux density can be changed by mechanical stress arising from the flow-induced vibration. According to Faraday's law of induction, the change in internal magnetic flux density over time caused by periodic bending deformation due to vibration generates a voltage in the coils. In the previous study, the effect of a splitter plate (SP) on the flow-induced vibration characteristics of cantilever rectangular prisms with different side ratios using wind tunnel experiments was investigated, and found that SP can stabilize the vibration amplitude [Hamano et. al., 2023].

In the present study, the effects of the height and the interior angle of V-shaped prisms having a span length of $L = 200$ mm on transverse vibration characteristics and power generation were investigated by the wind tunnel test. In addition, the present study aims to extend the steadiness of the response amplitude and reduce the velocity of oscillation onset of a V-shaped prism by putting

SP within the wake of the prism. Therefore, the effect of the gap, G , between SP and the prism on the transverse vibration characteristics of the cantilevered prisms was also investigated. In addition, the connection between flow patterns around the prism and vibrational properties is disclosed through flow visualizations employing a smoke wire method.

2. EXPERIMENTAL APPARATUS AND METHOD

Figure 1 shows a schematic diagram of the experimental setup. Experiments were conducted using a blow-down-type wind tunnel. The vibration-powered generator consists of a magnetostrictive material, an induction coil, a U-shaped frame, a permanent magnet, and a V-shaped prism. The frame and the magnetostrictive material have a unimorphic structure joined by an epoxy adhesive. The prism is allowed to vibrate transversely to the flow direction. Figure 2 shows the dimensions of the test models. The models were fabricated using a 3D printer using a filament of polylactic acid (PLA) resin. The models had a span length, L , of 200 mm, and a cross-sectional height H from 20 mm to 60 mm. An SP with a length of 400 mm and a thickness of 2 mm was installed behind the center of the prism with a gap varied from 8 to 104 mm. The vibration displacement, y , was measured with a laser displacement meter at a model height from the bottom edge of the prism, l , of 170 mm. The characteristic frequency, f_c , of the prism was measured by a fast Fourier transform analyzer. The reduced mass-damping parameter $C_n (= 2m\delta/\rho_{air}V_f)$ was measured considering the initial displacement obtained by hitting the test models in still air, where m , δ , ρ_{air} , and V_f are the mass of the prism, the logarithmic decay rate of the structural damping parameter of the prism, air density, and the volume of a prism, respectively. The uniform wind velocity, U , varied from 0.5 to 6.5 m/s. The generated power $P_{rms} [= V_{rms}^2/R]$, where V_{rms} is the generated voltage, and R is the resistance with a value of 400 Ω and the power coefficient $C_p [= P_{rms}/P_w]$, where $P_w (= 0.5\rho_{air}LHU^3)$ is the wind energy were calculated using a personal computer. Moreover, the flow around the V-shaped prism was visualized by the smoke, which was generated once an electric current from a transformer passed through two wires located upstream and downstream of the prism coated by fluid paraffin, which was captured by a high-speed camera.

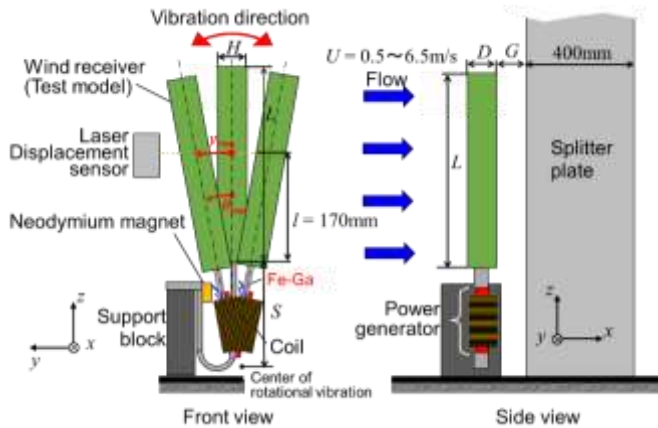


Fig.1 Schematic diagram of experimental setup

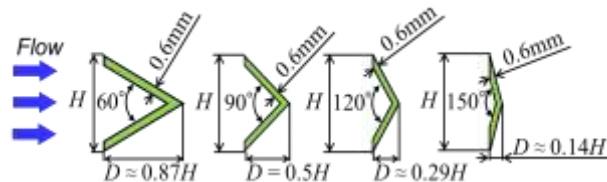


Fig.2 Test V-shaped prism

Table 1 Specifications of test prisms

(a) Without splitter plate ($\beta = 90^\circ$)

H [mm]	f_c [Hz]	δ
20	22.2	0.035
25	19.9	0.030
30	19.0	0.038
40	15.5	0.036
50	12.6	0.064
60	12.7	0.038

(c) With splitter plate ($H = 50$ mm and $\beta = 90^\circ$)

G/H	f_c [Hz]	δ
0.2	12.8	0.043
0.6	12.6	0.033
1.2	12.2	0.041
1.6	12.3	0.034
2.2	12.2	0.050
2.6	12.2	0.046
Without SP	12.6	0.064

(b) Without splitter plate ($H = 50$ mm)

β [deg.]	f_c [Hz]	δ
60	10.0	0.076
90	12.6	0.064
120	14.3	0.057
150	15.4	0.055

3. RESULTS AND DISCUSSION

(a) Effect of height H : Figure 3 shows the variation of the amplitude η_{rms} with the reduced velocity, $Vr (= U/f_c H)$, for a V-shaped prism having β of 90° without SP. The V-shaped prism is a soft oscillator and will gallop from rest at a flow velocity above a critical value [Parkinson, 1989]. The reduced velocity for vibration onset is $Vr \approx 4$, which is less than $Vr_{cr} \approx 7.94 (= 1/St, \text{ where } St \approx 0.126)$. Therefore, the V-shaped prism begins to vibrate by low-speed galloping. The maximum η_{rms} is 0.95 for $H = 30$ mm at $Vr = 7.58$. Although the prisms with $H = 20$ mm and 25 mm stops vibrating over $Vr \approx 8$, the prism with $H > 25$ mm continues vibration. Unfortunately, we ceased measuring the amplitude of prisms with $H > 25$ mm because the U-frame contacted the neodymium magnet due to the large oscillation.

(b) Effect of interior angle β : Figure 4 shows the variation of η_{rms} with Vr for V-shaped prisms with $H = 50$ mm at different interior angles β without SP. The value of the reduced velocity for vibration onset is decreasing with increasing the interior angle β . The prism having β of 60° occurs the divergent vibration where η_{rms} increases monotonically with increasing Vr due to high-speed galloping. It could be not a choice as an energy harvesting generator due to the safety point of view. In the case of the V-shaped prism having β of 120° , the value of η_{rms} of the prism increased abruptly and approached its maximum value of $\eta_{rms} \approx 0.46$ at $Vr \approx 5.8$, thereupon, the value of η_{rms} decreased gradually to stagnation at $Vr \approx 8.9$. The V-shaped prism having β of 150° starts to oscillate at $Vr \approx 4.7$ due to low-speed galloping and stops oscillation at $Vr \approx 8.5$. From the hysteresis phenomenon point of view, the variation of η_{rms} with Vr for the V-shaped prism having β of 150° has been affected by increasing or decreasing the flow velocity. As shown in Fig.5, comparing the results of trajectories of both tip edges of V-shaped prisms having β of 90° and 120° by the camera, it is clear that the free tip of the prism having β of 90° is more twisted near the maximum amplitude than that of the prism having β of 120° .

(c) Effect of installed splitter plate: Figure 6 shows the variation of η_{rms} with Vr for a V-shaped prism having β of 90° with SP. The prism with $G/H = 0.2$ did not vibrate without an added initial displacement. As shown in Fig. 7(a), the wake of a prism could not see the alternative vortex shedding due to the splitter plate. However, if the initial displacement was added to the prism, the vibration begins to occur near $Vr \approx 6.3$, and η_{rms} increases linearly with increasing reduced velocity until $Vr \approx 8$ ($\approx Vr_{cr}$). The onset velocity for a prism with $G/H = 0.6$ is $Vr \approx 3.9$, which is smaller than that for a prism without SP. The response amplitudes for prisms with $G/H = 1.2, 1.6, 2.2,$ and 2.6 are similar to that without SP. However, over the maximum peak of amplitude, the decrease in vibration amplitude is not very larger. Therefore, the splitter plate had little effect on the transverse vibration characteristics of a V-shaped prism. Figure 8 shows the variations of power generation P_{rms} and output coefficient C_p for V-shaped prism. The prism with $G/H = 1.2$ has $P_{rms \max} = 6.2$

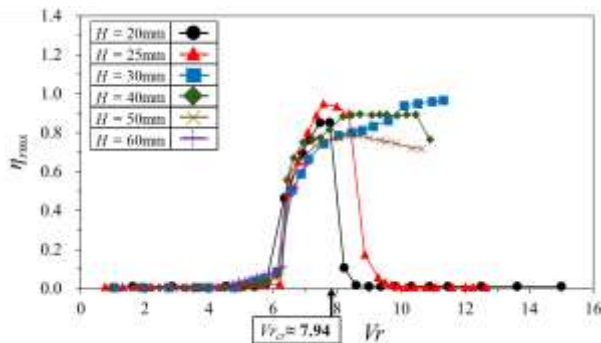


Fig. 3 Variation of response amplitude η_{rms} with reduced velocity Vr (Without SP)

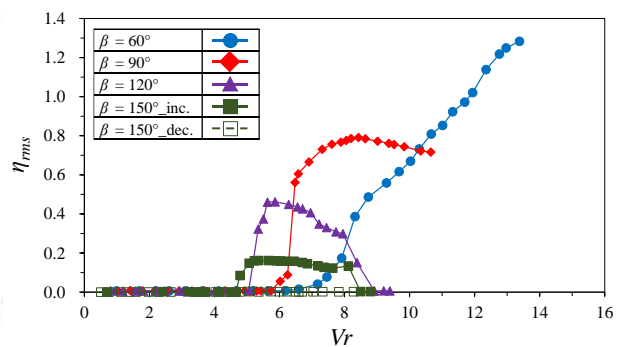


Fig. 4 Variation of response amplitude η_{rms} with reduced velocity Vr (Without SP)

mW ($U = 6.6$ m/s), and $C_p \max = 0.57\%$ ($U = 4.3$ m/s). Meanwhile, the prism without SP has $P_{rms \max} = 4.7$ mW ($U = 6.6$ m/s) and $C_p \max = 0.49\%$ ($U = 5.3$ m/s). These maximum power generations are enough to run a wireless sensor.

4. CONCLUSION:

The effects of an installed splitter plate, a height, and an interior angle of a V-shaped prism on the response characteristics and the power generation by the flow-induced vibration for a cantilevered V-shaped prism were investigated, and the flow around the prism was visualized by the smoke wire method. Although the prisms with $H = 20$ mm and 25 mm stop vibrating over $Vr \approx 8$, the prism with $H > 25$ mm continues vibration. The prism having $\beta = 90^\circ$ is more twisted near the maximum amplitude than that of the prism having $\beta = 120^\circ$. It is found that the splitter plate has little effect on the transverse vibration characteristics of a V-shaped prism with $G/H \geq 0.6$.

ACKNOWLEDGEMENTS

The present study was supported by MEXT JAPAN through the Program for Building Regional Innovation Ecosystems.

REFERENCES

- Hamano, T., Kiwata, T., Shima, T., Heragy, M. and Ueno, T., 2022. Proc. 7th Int. Conf. on Jets, Wakes and Separated Flows, D23, pp.1–6.
 Ueno, T. and Yamada, S., 2011. Performance of energy harvester using iron-gallium alloy in free vibration, IEEE Transactions on Magnetics 47, 2407–2409.
 Parkinson G., 1989. Phenomena and modeling of flow-induced vibrations of bluff bodies, Prog. Aerosp. Sci. 26, 169–224.

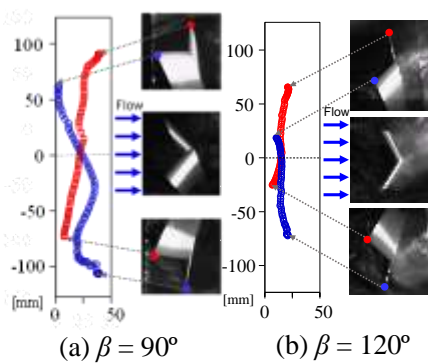
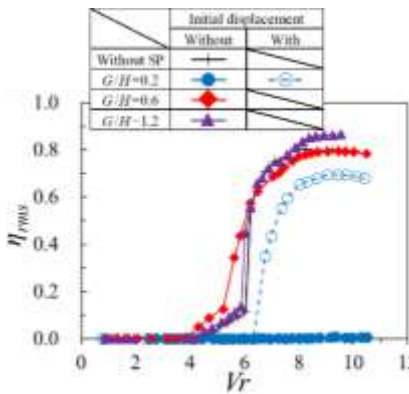
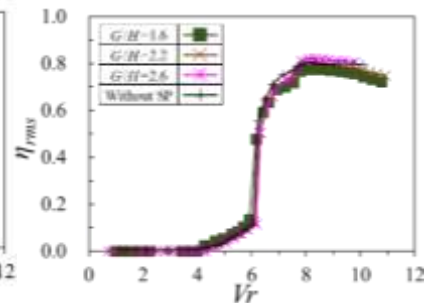


Fig.5 Trajectories of both tip edges of V-shaped prism at $U = 5$ m/s without SP



(a) $G/H = 0.2, 0.6, \text{ and } 1.2$



(b) $G/H = 1.6, 2.2, \text{ and } 2.6$

Fig.6 Variation of η_{rms} with Vr for a V-shaped prism with SP

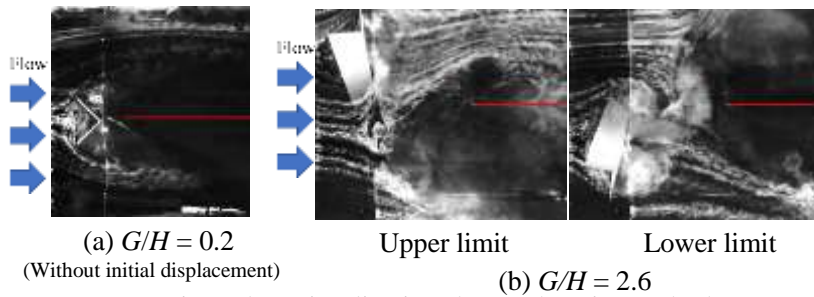


Fig.7 Flow visualizations by smoke wire method ($Vr \approx Vr_{cr}$, $U = 5.0$ m/s, With SP)

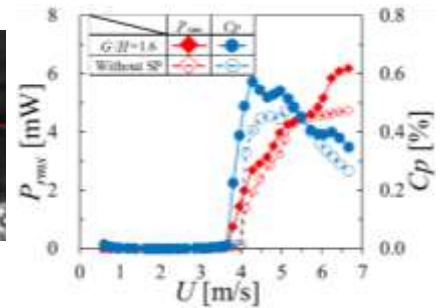


Fig.8 Variations of P_{rms} and C_p with flow velocity U